

Glycomic Analyses of Mouse Models of Congenital Muscular Dystrophy^{*[S]}

Received for publication, November 15, 2010, and in revised form, March 30, 2011. Published, JBC Papers in Press, April 1, 2011, DOI 10.1074/jbc.M110.203281

Stephanie H. Stalnak[‡], Kazuhiro Aoki[‡], Jae-Min Lim[‡], Mindy Porterfield[‡], Mian Liu[‡], Jakob S. Satz[§], Sean Buskirk[‡], Yufang Xiong[¶], Peng Zhang[¶], Kevin P. Campbell^{§1}, Huaiyu Hu[¶], David Live[‡], Michael Tiemeyer[‡], and Lance Wells^{‡2}

From the [‡]Complex Carbohydrate Research Center, University of Georgia, Athens, Georgia 30602-4712, the [§]Department of Molecular Physiology and Biophysics, Howard Hughes Medical Institute, Iowa City, Iowa 52242, and the [¶]State University of New York Upstate Medical University, Syracuse, New York 13210

Dystroglycanopathies are a subset of congenital muscular dystrophies wherein α -dystroglycan (α -DG) is hypoglycosylated. α -DG is an extensively *O*-glycosylated extracellular matrix-binding protein and a key component of the dystrophin-glycoprotein complex. Previous studies have shown α -DG to be post-translationally modified by both *O*-GalNAc- and *O*-mannose-initiated glycan structures. Mutations in defined or putative glycosyltransferase genes involved in *O*-mannosylation are associated with a loss of ligand-binding activity of α -DG and are causal for various forms of congenital muscular dystrophy. In this study, we sought to perform glycomic analysis on brain *O*-linked glycan structures released from proteins of three different knock-out mouse models associated with *O*-mannosylation (POMGnT1, LARGE (Myd), and DAG1^{-/-}). Using mass spectrometry approaches, we were able to identify nine *O*-mannose-initiated and 25 *O*-GalNAc-initiated glycan structures in wild-type littermate control mouse brains. Through our analysis, we were able to confirm that POMGnT1 is essential for the extension of all observed *O*-mannose glycan structures with β 1,2-linked GlcNAc. Loss of LARGE expression in the Myd mouse had no observable effect on the *O*-mannose-initiated glycan structures characterized here. Interestingly, we also determined that similar amounts of *O*-mannose-initiated glycan structures are present on brain proteins from α -DG-lacking mice (DAG1) compared with wild-type mice, indicating that there must be additional proteins that are *O*-mannosylated in the mammalian brain. Our findings illustrate that classical β 1,2-elongation and β 1,6-GlcNAc branching of *O*-mannose glycan structures are dependent upon the POMGnT1 enzyme and that *O*-mannosylation is not limited solely to α -DG in the brain.

Congenital muscular dystrophy (CMD)³ is a heterogeneous group of inherited neuromuscular disorders characterized by severe muscle weakness, ocular and neuronal migration abnormalities, and variable mental retardation (1). Within recent years, it has become increasingly clear through genetic studies that hypoglycosylation of the protein dystroglycan (DG) is a commonality in many forms of CMD (the so-called dystroglycanopathies). DG is post-translationally cleaved into an extracellular α -DG subunit and a transmembrane β -DG subunit (2). α -DG is a key component of the dystrophin-glycoprotein complex that serves as a link between the cytoskeleton of cells and the extracellular matrix by binding to proteins such as laminin (3). Interaction between α -DG and its extracellular ligands requires α -DG to be properly post-translationally modified through the addition of *O*-linked oligosaccharides, specifically *O*-mannose (4, 5). To date, mutations in six genes that encode determined or predicted glycosyltransferases have been shown to result in varying forms of CMD in which the post-translational processing of α -DG is affected (4–6). The six mutated genes and their original resulting form of CMD are as follows: *POMT1* (protein *O*-mannosyltransferase 1) and *POMT2*, Walker-Warburg syndrome (7, 8); *POMGnT1* (protein *O*-linked mannose β 1,2-*N*-acetylglucosaminyltransferase 1), muscle-eye-brain disease (9); *fukutin*, Fukuyama congenital muscular dystrophy (10); *FKRP* (*fukutin*-related protein), congenital muscular dystrophy 1C (11); and *LARGE*, congenital muscular dystrophy 1D (12). Recent work has demonstrated that selected mutations in some of these genes can cause various forms of CMD that are likely dependent on the severity of the mutation on enzymatic activity and stability (13). Abnormal glycosylation of α -DG appears to be a commonality among all of the aforementioned forms of CMD. Although expression of α -DG appears not to be grossly affected, the ability of α -DG to be recognized by monoclonal antibodies I1H6 and VIA4₁ is eliminated, as is the ability of α -DG to properly bind its ligands (14).

α -DG is composed of a central mucin-like region that is extensively heterogeneously glycosylated with glycan chains that are initiated by both *O*-GalNAc and *O*-mannose (15–17). POMT1, POMT2, and POMGnT1 have been shown to catalyze

* This work was supported, in whole or in part, by National Institutes of Health Grants HD060458 and NS066582 (to H. H.). This work was also supported by the Muscular Dystrophy Association (to L. W.), National Center for Research Resources Center Grant P41RR018502 (to L. W. and M. T.), and Senator Paul D. Wellstone Muscular Dystrophy Cooperative Research Center Grant 1U54NS053672 (to K. P. C.).

[S] The on-line version of this article (available at <http://www.jbc.org>) contains supplemental Figs. S1 and S2 and Table S1.

¹ Investigator of the Howard Hughes Medical Institute.

² To whom correspondence should be addressed: Complex Carbohydrate Research Center, University of Georgia, 315 Riverbend Rd., Athens, GA 30602-4712. Tel.: 706-542-7806; Fax: 706-542-4412; E-mail: lwells@ccrc.uga.edu.

³ The abbreviations used are: CMD, congenital muscular dystrophy; DG, dystroglycan; GFAP, glial fibrillary acidic protein; TIM, total ion mapping; Fmoc, *N*-(9-fluorenyl)methoxycarbonyl; HMBC, heteronuclear multiple-bond coherence.

the first two steps involved in the synthesis of a sialylated *O*-mannosyl tetrasaccharide structure (9, 18). The previously identified glycan structure Neu5Ac(α 2-3)Gal(β 1-4)GlcNAc(β 1-2)Man was identified on α -DG isolated from both brain and muscle and was previously thought to be required for ligand-binding activity. However, more recent studies have suggested that laminin binding is most likely not dependent on this structure, as treating α -DG with a series of glycosidases resulting in the trimming of this *O*-mannosyl tetrasaccharide structure does not abolish laminin-binding activity but rather enhances the ability of α -DG to bind to laminin (19). Additionally, recent work by Yoshida-Moriguchi *et al.* (20) has shown that LARGE, a putative glycosyltransferase, is involved in the synthesis of a rare extended phosphorylated *O*-mannosyl trisaccharide core structure on recombinant α -DG secreted from HEK293H cells, which is required for laminin binding. The roles that the other putative glycosyltransferases, fukutin and FKR, have in the post-translational processing of α -DG have yet to be determined.

Given the importance of post-translational processing of α -DG as related to CMD and the abundance of *O*-mannosyl glycan structures in the brain (~30% of *O*-glycan structures are *O*-mannose-initiated (21)), we sought to identify and characterize the relative abundance of *O*-glycan structures released from the mouse brain proteins of CMD disease models and their comparative wild-type controls. To do this, we implemented strategies that had been previously developed and described (22). Glycomic analysis of the various mouse models of CMD consisted of chemically releasing all *O*-glycans by reductive β -elimination, followed by permethylation and analysis by tandem mass spectrometry (23). From the implemented workflow, we were able to fully characterize many *O*-glycans released from mouse brain proteins of selected mouse models of CMD and to compare their relative abundances between the control and disease states. This study highlights the relative abundance of *O*-mannose- and *O*-GalNAc-initiated glycan structures characterized from the three CMD mouse brain models studied as well as the role of crucial enzymes and substrates in the *O*-mannosylation process.

EXPERIMENTAL PROCEDURES

Preparation of Whole Animal and Tissue-specific Knock-out Mouse Models of CMD—The whole body and tissue-specific knock-out mouse models of CMD were prepared as reported previously for POMGnT1, LARGE (Myd), and GFAP-DAG1 (24–26).

Preparation of Brain Protein Powder—Protein powder was prepared from the brains of various mouse models (postnatal days 2–7) of CMD as described previously (23). Briefly, to prepare protein powder from mouse brains, frozen brains were homogenized and delipidated in a solvent mixture with a final ratio of 4:8:3 chloroform/methanol/water. The extracted material was allowed to incubate for 6 h at room temperature. The precipitated protein material was collected by centrifugation, and the resulting protein pellet was re-extracted with fresh solvent. The precipitated protein pellet was washed with ice-cold 20% acetone and then dried under a gentle nitrogen stream at 45 °C.

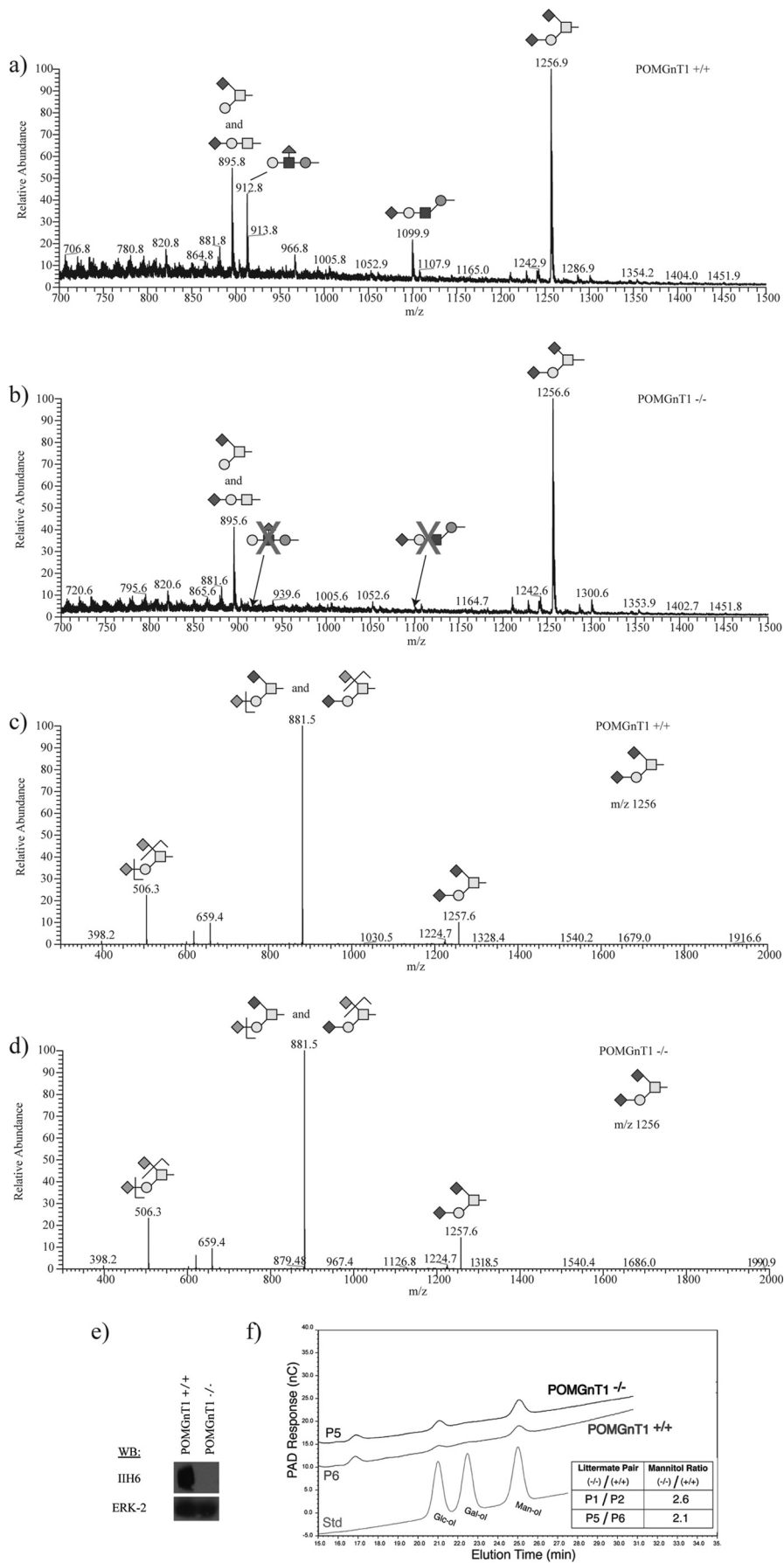
Release of O-Linked Glycans—*O*-Glycans were released using reductive β -elimination as reported previously (16). Briefly, protein powder was resuspended with 1 M NaBH₄ in 50 mM NaOH and incubated at 45 °C for 18 h. Following incubation, the reaction mixture was neutralized by adding 10% acetic acid dropwise while vortexing. The completely neutralized samples were desalted by loading onto a Bio-Rad AG-50W-X8 column (1-ml bed volume). The released oligosaccharides were eluted from the column with 3 volumes of 5% acetic acid and taken to dryness using a SpeedVac. Borate was removed by adding 10% acetic acid in methanol and drying under a nitrogen stream at 45 °C. All comparative analyses were conducted on equal amounts of protein.

Permethylation and Analysis of O-Glycans by Nanospray Ionization MS—Released oligosaccharides were permethylated to facilitate their analysis by mass spectrometry as reported previously (27). For analysis by nanospray ionization MS, permethylated glycans were dissolved in 1 mM NaOH in 50% methanol and directly infused into a linear ion trap mass spectrometer (LTQ, Thermo Scientific) at a flow rate of 0.4 ml/min. As described previously, the total ion mapping (TIM) function of the Xcalibur software package was used to detect and quantify the prevalence of all detected glycan structures (22). Through the application of TIM, MS/MS spectra were acquired within overlapping collection windows that span 2.8 mass units. This method was used to scan the *m/z* range from 200 to 2000. Following characterization of the *O*-glycan structures observed from the resulting TIM scan, the relative abundance of either individual glycans or groups of isobaric glycans was determined. The relative abundance of the observed glycan structures was calculated based upon the peak area from a single glycan structure relative to the total area of all observed *O*-glycan structures. Analyses of *O*-glycans released from both POMGnT1^{+/+} and POMGnT1^{-/-}, as well as LARGE^{+/+} and LARGE^{-/-}, were performed in triplicate, and differences in the relative abundance of these glycan structures is indicated, whereas those with α -DG^{+/+} and α -DG^{-/-} (GFAP-Cre/DAG1 knock-out) were performed only in duplicate, and the average value without S.D. is shown. Glycan nomenclature and representation of all glycan structures shown in the figures and tables are in agreement with the guidelines proposed by the Consortium of Functional Glycomics, with unidentified HexNAc residues displayed in gray.

Characterization of O-Mannitol by High Pressure Liquid Chromatography—Monosaccharides were released from both POMGnT1^{+/+} and POMGnT1^{-/-} mouse brain proteins (23), and the abundance of *O*-mannitol was analyzed (23) as described previously. Briefly, *O*-glycans were released from protein powder prepared from both POMGnT1^{+/+} and POMGnT1^{-/-} brains by reductive β -elimination, separated on a Dionex CarboPac MA-1 column (250 × 4 mm), and detected by high pH anion-exchange chromatography with pulsed amperometric detection. The detected monosaccharide peaks were later quantified based on monosaccharide alditol standards (note that glucitol levels are inherently difficult to measure by this method (23)).

Western Blotting—Mouse brain proteins from all three phenotypes were separated by SDS-PAGE on a 7.5% Tris-HCl pre-

O-Linked Glycans of Mouse Models of CMD



cast gel (Bio-Rad). Following separation, proteins were transferred to PVDF membranes using semidry transfer and probed using monoclonal antibody I1H6 (1:2000 dilution; Millipore) and anti-ERK2 antibody C-14 (1:5000 dilution; Santa Cruz Biotechnology) as a loading control. Proteins were detected using SuperSignal West Pico chemiluminescent substrate (Thermo Scientific).

Synthesis of Ac-Tyr-Val-Glu-Pro-Thr-(α -D-Man)-Ala-Val-NH₂—Peptide synthesis and preparation of Fmoc-Thr-(Ac₄- α -D-Man)-OH generally followed common synthesis methods. Peptide chain assembly starting with Fmoc-PAL-PEG-PSTM resin (0.3 g, 0.18 mmol/g; Applied Biosystems, Foster City, CA) was carried out manually. A Discover microwave reactor (CEM Corp., Matthews, NC) was used for accelerated deprotection and coupling reactions at elevated temperature. Side chain protection employed was *tert*-butyl for Tyr and *tert*-butyloxy for Glu. All reactions were carried out in a plastic vessel (25 ml) with a porous polypropylene frit, and no stirring was used. Fmoc removal was achieved with piperidine/*N,N*-dimethylformamide (1:4) for 4 min at 75 °C under 30-watt microwave irradiation, couplings (2.5 eq of Fmoc-amino acids) were mediated by 2-(1*H*-6-chlorobenzotriazol-1-yl)-1,1,3,3-tetramethyluronium hexafluorophosphate (2.5 eq)/1-hydroxybenzotriazole (2.5 eq)/*N,N'*-diisopropylethylamine (5 eq) for 9.5 min at 75 °C under 25-watt microwave irradiation, and *N*-acetyl capping was carried out with acetic anhydride/*N,N*-dimethylformamide (1:4) for 4 min at 75 °C under 30-watt microwave irradiation. The coupling of Fmoc-Thr-(Ac₄- α -D-Man)-OH (1.5 eq) was mediated by 2-(1*H*-6-chlorobenzotriazol-1-yl)-1,1,3,3-tetramethyluronium hexafluorophosphate (1.5 eq)/1-hydroxybenzotriazole (1.5 eq)/*N,N'*-diisopropylethylamine (3 eq) for 9.5 min at 75 °C under 25-watt microwave irradiation. Double couplings of Fmoc-Thr-(Ac₄- α -D-Man)-OH (0.5 eq), Fmoc-Pro-OH (2.5 eq), and Fmoc-Glu-*tert*-butyloxy-OH (2.5 eq) were carried out under the same microwave coupling conditions and with the corresponding amounts of 2-(1*H*-6-chlorobenzotriazol-1-yl)-1,1,3,3-tetramethyluronium hexafluorophosphate, 1-hydroxybenzotriazole, and *N,N'*-diisopropylethylamine. Approximately half of the peptide resin was treated with TFA/H₂O (19:1, 5 ml) in a glass flask (25 ml) with stirring for 2 h at 25 °C to cleave the Ac-YVEPT-(Ac₄- α -D-Man)-AV-NH₂ from the resin and to concurrently remove *tert*-butyl and *tert*-butyloxy side chain-protecting groups. The cleaved peptide/resin mixture was then washed extensively with TFA (3 × 1 ml), and the *O*-acetylated glycopeptide was precipitated by adding cold anhydrous ether (100 ml) to the combined filtrates. The ether-treated material was kept overnight at 4 °C and was then collected by centrifugation and washed further with cold ether (2 × 10 ml). The *O*-acetylated glycopeptide was purified by semipreparative reversed phase

HPLC, and the fractions with the desired products were pooled and lyophilized. The lyophilized *O*-acetylated glycopeptide was then dissolved in methanol (~4 ml/mg) for removal of *O*-acetyl groups. The pH of the methanol solution was adjusted to ~9 (as detected by wet litmus paper) by adding a solution of NaOMe in methanol. The *O*-deacetylation reaction was carried out with mild stirring and monitored by analytical reversed phase HPLC, going to completion after 5 h. Powdered CO₂ (dry ice) was then added carefully to reach a pH of 6, and the pure glycopeptide was obtained after semipreparative reversed phase HPLC, followed by lyophilization of the appropriate fractions. The amount obtained was 15 mg. The overall yield based on the initial substitution of resin was 57%. Electrospray ionization MS results were 981.4 [M + H]⁺ and 1003.4 [M + Na]⁺.

Enzymatic Synthesis of Ac-YVEP-(GlcNAc- β 1,2-Man- α)-TAV-NH₂—Ac-YVEP-(GlcNAc- β 1,2-Man- α)-TAV-NH₂ was prepared from Ac-YVEP-(Man- α)-TAV-NH₂ using the POMGnT1 enzyme. The DNA sequence for human POMGnT1 (provided by Dr. Huaiyu Hu, State University of New York) was cloned into a pSecTAG2B vector and stably transfected into HEK293 cells. For POMGnT1 purification, the culture medium was collected from the HEK-POMGnT1 cells and combined with a mixture of protease inhibitors. The medium was then chromatographed through a nickel chelating column, and the active glycosyltransferase was partially purified by elution with 300 mM imidazole at pH 6.8. To avoid aggregation and to stabilize the recombinant enzyme in solution, bovine serum albumin was usually added, and the resulting mixture was dialyzed (to remove the imidazole) and then concentrated. To assay the enzymatic activity, the incorporation of radiolabeled GlcNAc from UDP-[³H]GlcNAc into α 1-*O*-benzyl-Man was measured over time, and the reaction product was purified by solid phase extraction on a SepPak C₁₈ cartridge. In a typical purification procedure, 2–5 ml of a solution with partially pure enzyme could be obtained with an activity of 190 milliunits/ml. 0.8 mg of Ac-YVEP-(Man- α)-TAV-NH₂ was treated with recombinant POMGnT1 and UDP-GlcNAc, and the process was driven to completion over 72 h using buffer conditions as described above in the presence of alkaline phosphatase to prevent the accumulation of the glycosyltransferase inhibitor UDP. The monosaccharide- and disaccharide-substituted peptides were separated by analytical reversed phase HPLC on a C₁₈ column (4.6 × 250 mm) with detection at 220 nm and elution with 0.1% aqueous TFA (buffer A) and 0.1% TFA in CH₃CN (buffer B) and a linear gradient from 0 to 10% buffer B at a flow rate of 1 ml/min for 40 min.

NMR Studies—A sample of <1 mg of Ac-YVEP-(GlcNAc- β 1,2-Man- α)-TAV-NH₂ was dissolved in 90 μ l of D₂O in a 3-mm NMR microcell (Shigemi, Inc., Allison Park, PA). NMR spectra were obtained on a Varian NMRS 600-MHz

FIGURE 1. O-Glycans released from POMGnT1^{+/+} and POMGnT1^{-/-} mouse brain proteins. *a* and *b*, *O*-glycans were released from protein powder made from POMGnT1^{+/+} and POMGnT1^{-/-} mouse brain proteins by reductive β -elimination. Through comparison of the full MS scans of POMGnT1^{+/+} and POMGnT1^{-/-}, we were able to observe the absence of prominent *O*-mannose structures in POMGnT1^{-/-}. *c* and *d*, from the MS/MS scan (*m/z* 1256), the disialylated Tn antigen is unaffected in both POMGnT1^{+/+} and POMGnT1^{-/-}. *e*, antibody I1H6, which recognizes the fully glycosylated, functionally active form of α -DG, shows absence of functionally active α -DG in POMGnT1^{-/-} brains. *WB*, Western blot. *f*, individual monosaccharides were released from both POMGnT1^{+/+} and POMGnT1^{-/-} mouse brain proteins, and the relative abundances of *O*-mannitol were compared. From the two data sets, proteins carrying non-extended *O*-mannose structures were determined to be enriched by ~2.4-fold in the POMGnT1^{-/-} animals. *PAD*, pulsed amperometric detection; *Std*, standard.

O-Linked Glycans of Mouse Models of CMD


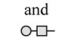

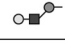
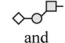

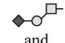


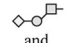
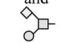


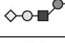



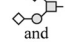


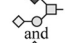



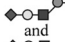


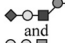






NMR spectrometer with a 3-mm HCN cold probe. ^1H double-quantum filtered COSY, ^1H total correlation spectroscopy, ^1H - ^{13}C gradient heteronuclear multiple-quantum coherence, and ^1H - ^{13}C gradient heteronuclear multiple-bond coherence (HMBC) data were recorded using the standard pulse sequences in Vnmrj software and were processed on the spectrometer. From these data, all resonances were assigned for the disaccharide glycan, and connectivities across the glycosidic linkages were established with the HMBC experiment.

RESULTS

POMGnT1 Is Required for the Extension of O-Mannose by β 1,2-Linked GlcNAc—O-Linked glycans were released from both POMGnT1^{+/+} and POMGnT1^{-/-} mouse brain proteins by reductive β -elimination and then permethylated to facilitate their analysis by nanospray ionization MS/MS. The acquired full MS scans (m/z 700–1500) (Fig. 1, *a* and *b*) allowed for the detection of O-glycan structures released from both POMGnT1^{+/+} and POMGnT1^{-/-} mouse brain proteins. The structural assignment of O-glycans observed in the full MS scans was based upon subsequent MS/MS fragmentation data. To detect all of the released O-glycan structures, we used TIM methodologies as described previously (22). By using TIM, we were able to acquire MS/MS fragmentation profiles allowing for the detection of O-glycans over the entire scanned m/z range. Fig. 1 (*c* and *d*) shows the MS/MS fragmentation profile of disialylated T antigen (m/z 1256) detected in both POMGnT1^{+/+} and POMGnT1^{-/-}. Table 1 contains a list of all glycan structures detected in both POMGnT1^{+/+} and POMGnT1^{-/-}. Fragmentation of extended O-mannose structures was not observed in POMGnT1^{-/-} (the glycan prevalence is indicated as “ND” (not detected) in Table 1 for all extended O-mannose structures). Additionally, mouse brain proteins from both POMGnT1^{+/+} and POMGnT1^{-/-} were separated by SDS-PAGE and probed with monoclonal antibody IIH6 (Fig. 1*e*), which detects fully glycosylated, functionally active α -DG. From the Western blot, we observed a loss of reactivity of IIH6 with proteins from POMGnT1^{-/-}, indicating that α -DG is hypoglycosylated and no longer functionally active. Through high pH anion-exchange chromatography with pulsed amperometric detection of β -eliminated reduced monosaccharide alditols from both POMGnT1^{+/+} and POMGnT1^{-/-} mouse brain proteins (equal amounts based on protein content), Man-ol was shown to be elevated by ~2.4-fold in POMGnT1^{-/-} compared with the POMGnT1^{+/+} littermate control (Fig. 1*f*), suggesting that POMT1/2 activity was unaffected.

As GlcNAc extension on O-mannose has recently been observed on α -DG in a β 1,4-linkage (20), we wanted to confirm the previous work by others that had demonstrated that POMGnT1 extends O-mannose in a β 1,2-linkage. Thus, we used recombinant POMGnT1 and UDP-GlcNAc to extend a synthetic O-mannose peptide and, following purification by reversed phase HPLC, analyzed the peptide by NMR techniques. The assignments of the resonance positions for all ^1H and ^{13}C NMR signals arising from the GlcNAc-Man disaccharide glycan on the glycopeptide Ac-YVEP-(GlcNAc- β 1,2-Man- α)-TAV-NH₂ (residues 410–416 of α DG), prepared

TABLE 1
O-Glycans released from POMGnT1^{+/+} and POMGnT1^{-/-} mouse brain proteins
ND, not detected.

No.	Structure	MW	POMGnT1 ^{+/+}	POMGnT1 ^{-/-}
1		534.3	11.9% ± 1.1%	ND
2				13.9% ± 4.9%
3		575.3	1.7% ± 0.5%	2.5% ± 1.1%
4		738.4	2.1% ± 0.4%	ND
5		867.5	2.0% ± 1.0%	3.9% ± 3.5%
6				
7		895.5	15.2% ± 0.2%	17.1% ± 4.6%
8				
9		912.5	7.5% ± 3.8%	ND
10		925.5	2.1% ± 0.5%	2.8% ± 0.9%
11				
12		983.5	0.9% ± 0.2%	1.3% ± 0.5%
13		1099.6	5.8% ± 1.6%	ND
14		1129.6	0.7% ± 0.1%	ND
15		1157.6	0.7% ± 0.04%	0.8% ± 0.2%
16		1187.6	0.9% ± 0.1%	0.9% ± 0.3%
17				
18		1228.6	2.5% ± 2.3%	8.4% ± 7.1%
19				
20		1256.6	40.0% ± 5.3%	41.7% ± 10.3%
21		1286.6	1.6% ± 0.5%	2.1% ± 0.3%
22				
23		1314.7	0.9% ± 1.1%	0.5% ± 0.1%
24		1316.7	0.4% ± 0.04%	0.5% ± 0.2%
25		1344.7	0.9% ± 0.2%	ND
26				1.1% ± 0.2%
27		1501.8	0.1% ± 0.01%	0.3% ± 0.04%
28		1548.8	0.3% ± 0.1%	ND
29				0.6% ± 0.3%
30		1617.8	1.1% ± 0.3%	1.1% ± 0.3%
31		1705.9	0.2% ± 0.02%	0.3% ± 0.2%
32		1722.9	0.2% ± 0.02%	ND
33				0.1% ± 0.04%
34		1910.0	0.2% ± 0.02%	ND

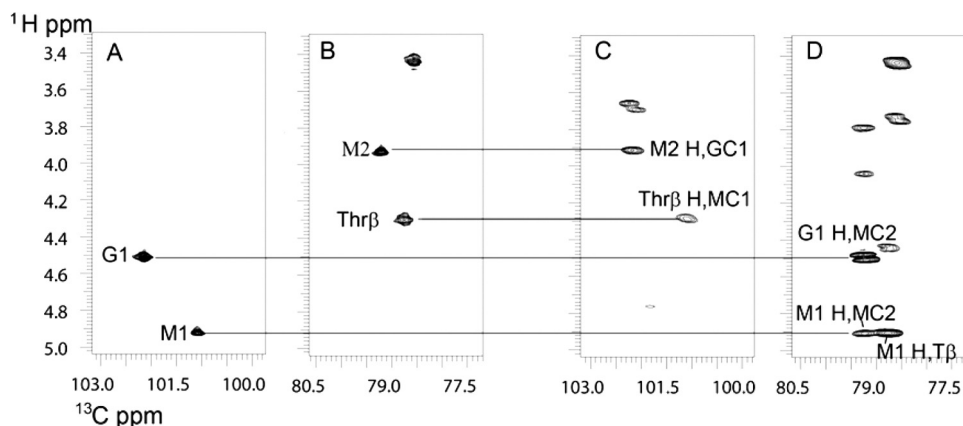


FIGURE 2. **Linkage analysis of recombinant POMGnT1 by NMR.** Two-dimensional ^1H - ^{13}C correlation spectra show signals derived from the carbohydrate portion of the Ac-YVEP-(GlcNAc- β 1,2-Man- α)-TAV-NH₂ glycopeptide prepared from POMGnT1 action on the mannosylated peptide. A and B, sections from a heteronuclear multiple-quantum coherence spectrum, where the cross-peaks are at the coordinates of pairs of directly bonded protons and carbons. C and D, similar regions from the HMBC spectrum, where the peaks are at the coordinates of a proton and carbons two or three bonds away. The lines correlate peaks in the spectra that derive from the same protons associated with respective glycosidic linkages. Peaks in C show connections between the H-2 proton of Man and C-1 of GlcNAc, establishing the GlcNAc C-1 to Man C-2 glycosidic linkage, and additionally the linkage from the Thr- β proton to Man C-1. These are confirmed in the other direction across the linkages by the peaks in D.

by recombinant POMGnT1 enzymatic addition of GlcNAc to the Man glycopeptide, were made using homonuclear two-dimensional ^1H double-quantum COSY and total correlation spectroscopy experiments and ^1H - ^{13}C heteronuclear multiple-quantum coherence and HMBC two-dimensional correlations. The latter experiment shows correlations between ^1H and ^{13}C nuclei with two or three intervening bonds (28), allowing explicit connections to be established across the glycosidic linkages. The initial identification of the Man- α and the GlcNAc- β anomeric sites could be readily made based on the distinct ^1H and ^{13}C carbon shift positions associated with their respective stereochemistry (29, 30). Furthermore, the $^3J_{\text{H1-H2}}$ couplings for the anomeric protons were as predicted for the linkage stereochemistry, with a large coupling of ~ 8.5 Hz in the one-dimensional ^1H spectrum clearly showing the GlcNAc linkage to be β (30). The locations of the Man anomeric signals were also in agreement with that observed for the synthetic substrate glycopeptide Ac-YVEP-(Man- α)-TAV-NH₂ (data not shown). Using correlations that could be traced back to the assigned anomeric resonances, shifts for nuclei at the additional sites in each residue were determined with information derived from the experiments above (supplemental Figs. S1 and S2 and Table S1). Based on these assignments, HMBC cross-peaks arising from ^1H and ^{13}C connectivities in both directions across the glycosidic linkages between the sugar residues and from Man to Thr- β (Fig. 2) were identified. These results unequivocally establish the formation of a β 1,2-linkage between the GlcNAc and Man residues mediated by POMGnT1.

O-Glycans Released from and Detected in LARGE^{+/+} Versus LARGE^{-/-} Are Identical—O-Linked glycans were released from LARGE^{+/+} and LARGE^{-/-} (*myd1*) mouse brain proteins as described previously. Full MS scans (m/z 700–1500) (Fig. 3, a and b) of the released O-glycans indicated the most abundant glycan structures found in both the LARGE^{+/+} and LARGE^{-/-} samples to be similar. Structural analysis of the released O-glycans was based upon the acquired MS/MS fragmentation data. Fig. 3 (c and d) shows that synthesis of the O-mannosyl tetrasaccharide structure remained unaffected in LARGE^{-/-} based

upon structural assignment of characteristic fragments. The prevalence of all the characterized glycan structures was quantified using TIM, and no statistically relevant changes were observed (Table 2). Brain proteins from both LARGE^{+/+} and LARGE^{-/-} mice were separated by SDS-PAGE and probed with monoclonal antibody IIH6 (Fig. 3e). From the Western blot, we observed a loss of reactivity of IIH6 with proteins from LARGE^{-/-}, indicating that α -DG is hypoglycosylated and no longer functionally active.

O-Mannose-initiated Glycan Structures Are Still Detectable in α -DG^{-/-} Brain—As described above, O-glycans were released from α -DG^{+/+} and α -DG^{-/-} (GFAP-Cre/DAG1) mouse brain proteins. Full scans were acquired (m/z 700–1500) of released O-glycans from both α -DG^{+/+} and α -DG^{-/-} mouse brain proteins, with the most abundant glycan structures shown (Fig. 4, a and b). Through the MS/MS fragmentation spectra, we were able to confirm the presence of a fucosylated O-mannose trisaccharide isolated from the mouse brain proteins of both α -DG^{+/+} and α -DG^{-/-} (Fig. 4, c and d). Brain proteins from both LARGE^{+/+} and LARGE^{-/-} mice were separated by SDS-PAGE and probed with monoclonal antibody IIH6 (Fig. 4e). From the Western blot, we observed a substantial loss of reactivity of IIH6 with proteins from α -DG^{-/-}, indicating the absence of functionally active α -DG. Presumably, the weak band present in the knock-out results from endothelial, smooth muscle, and/or other non-neuronal cells in the brain tissue, where the dystroglycan gene would still be present and expressed in the neural specific knock-out animal used.

DISCUSSION

Hypoglycosylation of α -DG through genetic mutations has been shown to result in various phenotypes of CMD in which the post-translational processing of α -DG is affected, preventing binding to proteins of the extracellular matrix such as laminin, perlecan, and agrin (31). Proper glycosylation of α -DG is also essential for it to serve as a receptor for lymphocytic choriomeningitis virus, Lassa fever virus, and clade C New World arenaviruses (32, 33). To date, quantitative comparative

O-Linked Glycans of Mouse Models of CMD

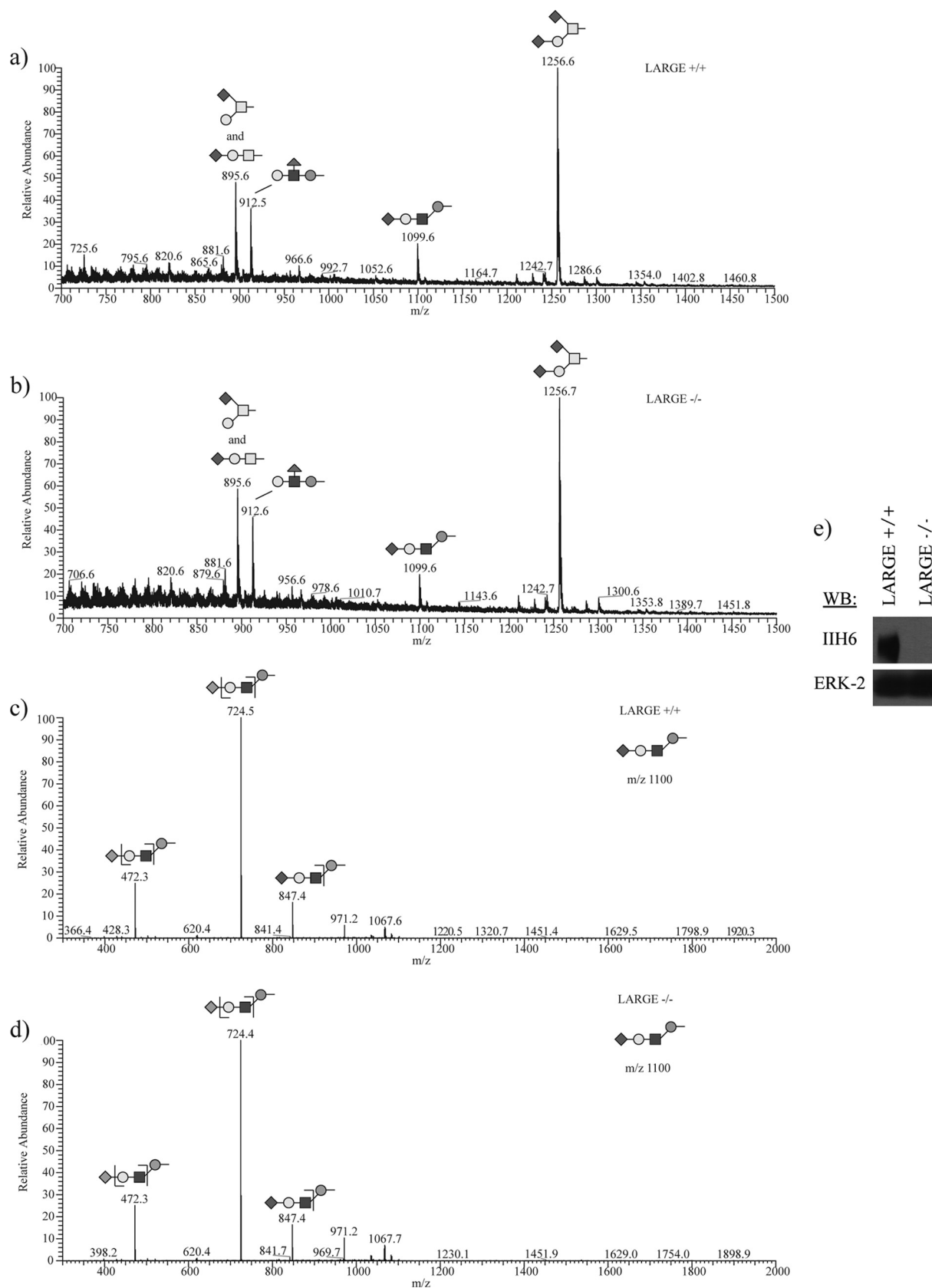

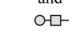


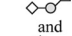
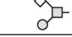
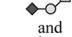
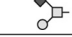

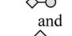
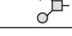
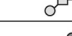



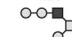



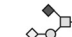


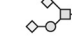
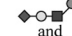
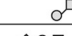

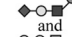
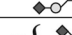

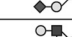
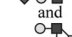
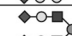
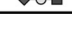



FIGURE 3. O-Glycans released from LARGE^{+/+} and LARGE^{-/-} mouse brain proteins. *a* and *b*, O-glycans were released from protein powder made from LARGE^{+/+} and LARGE^{-/-} mouse brain proteins. Through comparison of the full MS scans, we observed no difference in the prominent O-glycan structures that were detected in LARGE^{+/+} and LARGE^{-/-} mouse brain proteins. *c* and *d*, MS/MS fragmentation spectra (*m/z* 1100) indicate the presence of the classical O-Man tetrasaccharide in both the LARGE^{+/+} and LARGE^{-/-} mouse brains. *e*, antibody IIH6, which recognizes the fully glycosylated, functionally active form of α -DG, shows absence of functionally active α -DG in LARGE^{-/-} brains. WB, Western blot.

TABLE 2

O-Glycans released from LARGE^{+/+} and LARGE^{-/-} mouse brain proteins

No.	Structure	MW	LARGE ^{+/+}	LARGE ^{-/-}
1		534.3	24.9% ± 12.8%	23.2% ± 13.4%
2				
3		575.3	2.0% ± 0.4%	1.7% ± 0.4%
4		738.4	2.8% ± 0.2%	2.6% ± 0.2%
5		867.5	1.5% ± 0.4%	2.1% ± 1.2%
6				
7		895.5	15.9% ± 0.1%	15.6% ± 0.6%
8				
9		912.5	9.8% ± 0.9%	11.4% ± 1.9%
10		925.5	2.3% ± 0.6%	2.6% ± 0.3%
11				
12		983.5	0.8% ± 0.2%	0.9% ± 0.2%
13		1099.6	5.6% ± 1.8%	6.2% ± 1.9%
14		1129.6	0.6% ± 0.1%	0.8% ± 0.4%
15		1157.6	0.8% ± 0.3%	0.8% ± 0.3%
16		1187.6	0.6% ± 0.02%	0.6% ± 0.3%
17				
18		1228.6	1.6% ± 0.6%	1.7% ± 0.5%
19				
20		1256.6	26.2% ± 9.7%	25.6% ± 8.0%
21		1286.6	1.3% ± 0.4%	1.5% ± 0.4%
22				
23		1314.7	0.2% ± 0.1%	0.2% ± 0.1%
24		1316.7	0.4% ± 0.1%	0.4% ± 0.2%
25		1344.7	0.9% ± 0.2%	0.9% ± 0.2%
26				
27		1501.8	0.1% ± 0.02%	0.1% ± 0.07%
28		1548.8	0.3% ± 0.1%	0.2% ± 0.1%
29				
30		1617.8	0.7% ± 0.4%	0.6% ± 0.03%
31		1705.9	0.2% ± 0.1%	0.2% ± 0.07%
32		1722.9	0.2% ± 0.1%	0.2% ± 0.1%
33				
34		1910.0	0.2% ± 0.1%	0.2% ± 0.1%

studies of O-glycans released from models of CMD have yet to be conducted. Thus, we sought to characterize and quantify the structure and prevalence of the various O-glycans released from mouse brain proteins of three models of CMD.

O-Glycans were chemically released from brain proteins of POMGnT1^{-/-}, LARGE^{-/-}, and α -DG^{-/-} mice as well as their comparative wild-type littermates by reductive β -elimination. We started by comparing the full MS scans of O-glycans released from knock-out mouse brains with those of their wild-type littermates (Figs. 1, *a* and *b*; 3, *a* and *b*; and 4, *a* and *b*). Previous studies have shown that mutations in POMGnT1 prevent the extension of O-mannosyl glycans with GlcNAc residues (34). We were able to confirm the absence of extended O-mannosyl glycans in POMGnT1^{-/-} as shown in Table 1. Interestingly, no β 1,6-branching was observed, suggesting that the activity of POMGnT1 precedes and is necessary for the activity of GlcNAc transferase-Vb that is involved in branching of O-mannose structures (35). However, the presence of O-mannitol was elevated by \sim 2.4-fold in the brain tissue of POMGnT1^{-/-} compared with POMGnT1^{+/+}, suggesting no defect in POMT1/2 activity. Structural assignment made based upon acquired MS/MS fragmentation spectra further suggested that O-GalNAc-initiated glycans were unaffected (Fig. 1, *c* and *d*). Using antibody I1H6, which specifically recognizes functionally active, fully glycosylated α -DG, we detected the absence of functional α -DG in the POMGnT1^{-/-} brain, as expected.

Although POMGnT1 had previously been reported to extend O-mannosyl glycans with a β 1,2-linked GlcNAc residue (36), the presence of O-mannosyl glycans on α -DG extended with β 1,4-GlcNAc has recently been proposed (20). Prior work completed to determine the linkage of GlcNAc concluded that the GlcNAc residue was linked to C-2 of the mannose based upon treatment of released glycans with jack bean β -N-acetylhexosaminidase, which cleaves at the β 1,2-linkage. Additionally, analysis by reversed phase HPLC was used to confirm the extension of the O-mannose by β 1,2-linked GlcNAc (9). However, recent work by Yoshida-Moriguchi *et al.* (20) indicates the presence of a novel phosphorylated structure in which the O-mannose is extended by a β 1,4-linked GlcNAc. Therefore, we definitively determined the linkage at which GlcNAc was added to a synthetic O-mannosyl peptide with recombinant POMGnT1 using NMR. From our analysis, we concluded the POMGnT1 is indeed responsible for extending O-mannose with a β 1,2-linked GlcNAc (Fig. 2), as reported previously (36). This suggests that there is a yet undetermined GlcNAc-transferase capable of acting on O-mannose residues to introduce a β 1,4-linked GlcNAc moiety. Identification of the gene encoding this enzymatic activity could aid in diagnosing CMD patients because the majority have no established genetic etiology.

In our analysis of O-glycans released from LARGE^{+/+} and LARGE^{-/-} mouse brain proteins, we were unable to detect any differences in the relative abundance of observed O-glycan structures. However, previous work has shown α -DG to be hypoglycosylated in the LARGE-deficient myodystrophy (LARGE^{myd}) mouse, resulting in a reduction in ligand-binding activity (14). In work previously reported by Sutton-Smith *et al.*

O-Linked Glycans of Mouse Models of CMD

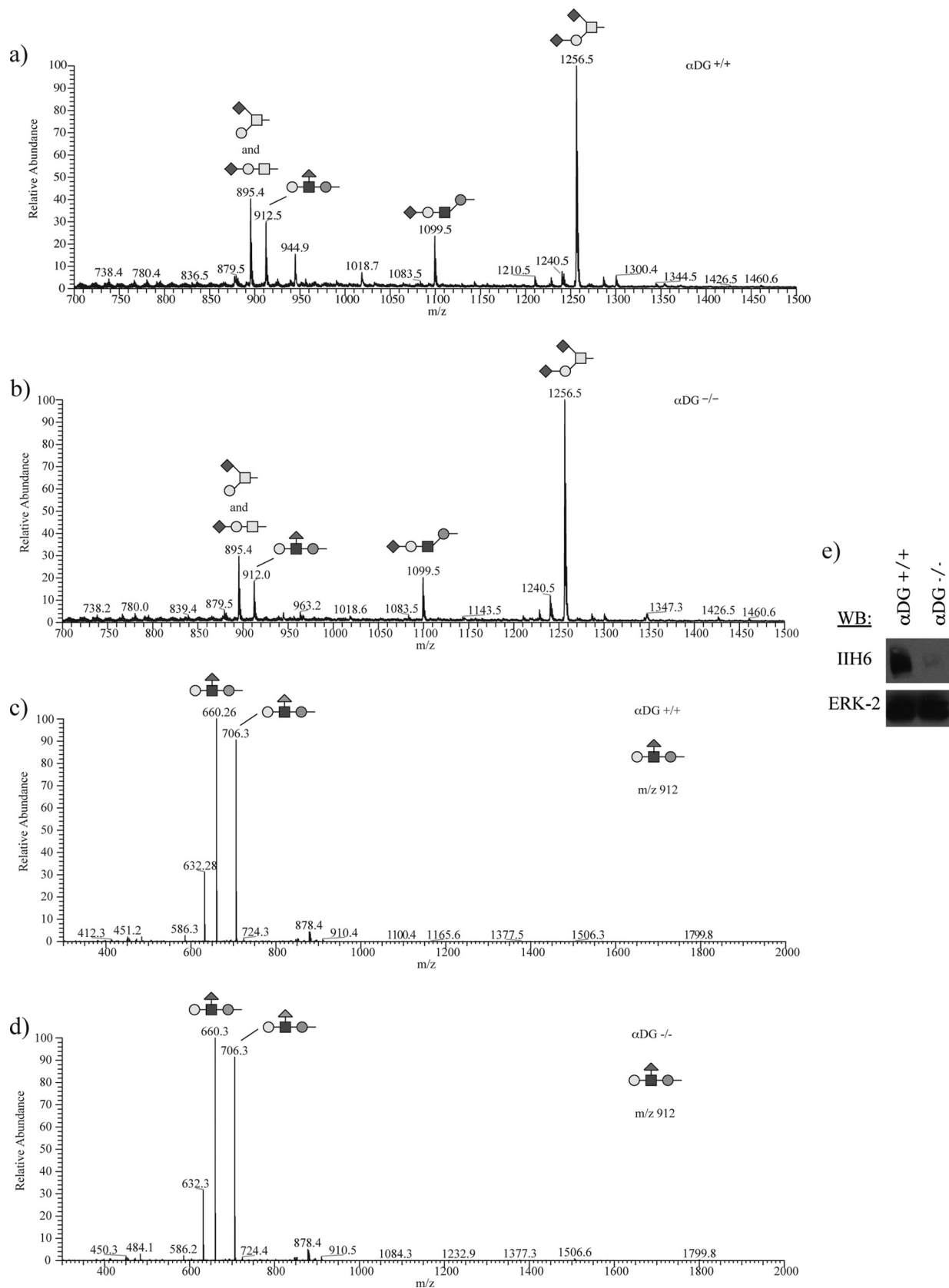


FIGURE 4. O-Glycans released from α -DG $^{+/+}$ and α -DG $^{-/-}$ (GFAP-Cre/DAG1) mouse brain proteins. *a* and *b*, O-glycans were released from protein powder of α -DG $^{+/+}$ and α -DG $^{-/-}$ cerebri. Through comparison of the full scan, we observed no difference in the amount of prominent O-mannose-initiated glycan structures detected in the α -DG $^{+/+}$ and α -DG $^{-/-}$ proteins. *c* and *d*, MS/MS fragmentation spectra (*m/z* 912) indicate the presence of the fucosylated O-mannose trisaccharide structure in both the α -DG $^{+/+}$ and α -DG $^{-/-}$ mouse brains. *e*, antibody I1H6, which recognizes the fully glycosylated, functionally active form of α -DG, indicates an order of magnitude decrease in the amount of α -DG levels present in the α -DG $^{-/-}$ brain compared with the α -DG $^{+/+}$ brain. *WB*, Western blot.

(37), O-glycan profiles from both normal and LARGE^{myd} mouse brains were compared. In their study, they observed three O-GalNAc-initiated and two O-mannose-initiated glycan structures of similar abundance in both the normal and LARGE^{myd} mouse brains. Here, we corroborated their findings with more in-depth analysis with our assignment of 25 O-GalNAc structures and nine O-mannose structures in both the LARGE^{+/+} and LARGE^{-/-} brains with similar abundances. Recently, Campbell and co-workers (20) observed a phosphorylated O-mannosyl glycan structure (which is LARGE-dependent) present on α -DG that is required for laminin binding. However, during our analysis of O-glycans released from LARGE^{-/-} mouse brain proteins, we were unable to observe this glycan structure (a phosphorylated trisaccharide). Most likely, the absence of this glycan structure in the LARGE^{-/-} brains can be attributed to its minor contribution to the complete pool of O-glycans and perhaps may reflect that it is on a limited set of proteins that include α -DG. In wild-type animals, we would expect this mannose-phosphorylated trisaccharide to be extended from the phosphate with an unknown moiety (20) and, as expected, were unable to detect it during our analysis.

Having fully characterized O-glycans from two mouse models of CMD, we proceeded to characterize O-glycans released from α -DG^{+/+} and α -DG^{-/-} mouse brain proteins because α -DG is the primary protein substrate associated with CMD and the only well characterized O-mannose-modified mammalian protein. Similar to the other instances in which we analyzed the released O-glycans, we proceeded to compare the relative abundance of O-glycans detected from both the wild-type and knock-out mouse brain proteins. Notably, from the generated full MS scans (Fig. 4, *a* and *b*), there was not a discernable difference in the prevalence of O-mannose-initiated glycan structures (Table 3) observed in the α -DG^{-/-} brain compared with those detected in the wild-type brain. The presence of O-mannosyl glycans was further confirmed upon analysis of the MS/MS fragmentation spectra as shown in Fig. 4 (*c* and *d*), where the presence of a fucosylated O-mannosyl glycan was confirmed in both the wild-type and α -DG^{-/-} brains. Consequently, we observed a significant reduction in the amount of α -DG detectable by Western blotting with antibody IIH6 against proteins from the α -DG^{-/-} brain (Fig. 4*e*). Our results mimic those obtained by Campbell and co-workers (26), where minute amounts of α -DG (<5% wild-type levels) could be detected in the vascular smooth muscle of cerebral blood vessels in the α -DG^{-/-} whole brain extract given that knock-out of the floxed *Dag1* gene was facilitated by breeding with GFAP-Cre animals. Comparison of the relative amounts of O-mannosyl glycans expressed on α -DG^{+/+} and α -DG^{-/-} mouse brain proteins demonstrates no significant difference in the amount of O-mannose structures attached to brain proteins, although α -DG expression was greatly reduced. This is strong evidence for the presence of additional O-mannose-modified proteins in the mammalian brain to explain O-mannose-initiated structures accounting for approximately one-third of all O-glycans released from proteins in brains from α -DG^{-/-} mice.

In conclusion, we were able to develop and implement workflows that allowed us to perform glycomic analysis on O-glycans released from the mouse brain proteins from select mouse

TABLE 3

O-Glycans released from wild-type and GFAP-Cre/DG null mouse cerebrum proteins

No.	Structure	MW	α DG +/+	α DG -/-
1		534.3	9.4%	11.4%
2	and 			
3		575.3	1.9%	2.1%
4		738.4	0.9%	1.5%
5		867.5	0.5%	0.9%
6	and 			
7		895.5	12.9%	12.6%
8	and 			
9		912.5	7.5%	6.9%
10		925.5	1.0%	1.1%
11	and 			
12		983.5	0.4%	0.5%
13		1099.6	8.5%	8.2%
14		1129.6	0.4%	0.7%
15		1157.6	0.6%	0.6%
16		1187.6	0.4%	0.6%
17	and 			
18		1228.6	1.7%	1.9%
19	and 			
20		1256.6	48.1%	45.4%
21		1286.6	1.7%	1.6%
22	and 			
23		1314.7	0.2%	0.2%
24		1316.7	0.3%	0.2%
25		1344.7	0.7%	0.7%
26	and 			
27		1501.8	0.2%	0.2%
28		1548.8	0.3%	0.4%
29	and 			
30		1617.8	1.3%	1.2%
31		1705.9	0.2%	0.2%
32		1722.9	0.3%	0.3%
33	and 			
34		1910.0	0.7%	0.6%

models involved in O-mannosylation. Collectively, we were able to fully characterize 34 different glycan structures from the three phenotypes and the wild-type controls we investigated (Tables 1–3). Through our analysis, we were able to identify nine O-mannose-initiated and 25 O-GalNAc-initiated (including six isobaric species) O-glycan structures. It should be noted, by comparing Tables 1–3, that the percentage of various glycan structures changed among the various wild-type controls, which likely reflects slight differences in mouse strains, age at analysis, and environments. By characterizing these O-glycan structures, we were able to provide some insight into the roles the known and putative glycosyltransferases POMGnT1 and LARGE, respectively, have in the O-mannosylation pathway, including providing conclusive evidence that POMGnT1 is essential for β 1,2-extension of O-Man with GlcNAc. Additionally, through the detection of O-mannosyl glycan structures in α -DG^{-/-}, we were able to provide conclusive evidence for additional O-mannosylated proteins being present in the mammalian brain.

Acknowledgments—We thank the members of the Tiemeyer and Wells' laboratory and Carl Bergmann for helpful advice and discussions and Michael Pierce's laboratory for graciously providing recombinant enriched POMGnT1.

REFERENCES

- Lisi, M. T., and Cohn, R. D. (2007) *Biochim. Biophys. Acta* **1772**, 159–172
- Ibraghimov-Beskrovnaya, O., Ervasti, J. M., Leveille, C. J., Slaughter, C. A., Sernett, S. W., and Campbell, K. P. (1992) *Nature* **355**, 696–702
- Ervasti, J. M., and Campbell, K. P. (1993) *J. Cell Biol.* **122**, 809–823
- Barresi, R., and Campbell, K. P. (2006) *J. Cell Sci.* **119**, 199–207
- Martin, P. T. (2007) *Curr. Mol. Med.* **7**, 417–425
- Endo, T., and Manya, H. (2006) *Methods Mol. Biol.* **347**, 43–56
- Beltrán-Valero de Bernabé, D., Currier, S., Steinbrecher, A., Celli, J., van Beusekom, E., van der Zwaag, B., Kayserili, H., Merlini, L., Chitayat, D., Dobyns, W. B., Cormand, B., Lehesjoki, A. E., Cruces, J., Voit, T., Walsh, C. A., van Bokhoven, H., and Brunner, H. G. (2002) *Am. J. Hum. Genet.* **71**, 1033–1043
- van Reeuwijk, J., Janssen, M., van den Elzen, C., Beltrán-Valero de Bernabé, D., Sabatelli, P., Merlini, L., Boon, M., Scheffer, H., Brockington, M., Muntoni, F., Huynen, M. A., Verrips, A., Walsh, C. A., Barth, P. G., Brunner, H. G., and van Bokhoven, H. (2005) *J. Med. Genet.* **42**, 907–912
- Yoshida, A., Kobayashi, K., Manya, H., Taniguchi, K., Kano, H., Mizuno, M., Inazu, T., Mitsuhashi, H., Takahashi, S., Takeuchi, M., Herrmann, R., Straub, V., Talim, B., Voit, T., Topaloglu, H., Toda, T., and Endo, T. (2001) *Dev. Cell* **1**, 717–724
- Kobayashi, K., Nakahori, Y., Miyake, M., Matsumura, K., Kondo-Iida, E., Nomura, Y., Segawa, M., Yoshioka, M., Saito, K., Osawa, M., Hamano, K., Sakakihara, Y., Nonaka, I., Nakagome, Y., Kanazawa, I., Nakamura, Y., Tokunaga, K., and Toda, T. (1998) *Nature* **394**, 388–392
- Brockington, M., Blake, D. J., Prandini, P., Brown, S. C., Torelli, S., Benson, M. A., Ponting, C. P., Estournet, B., Romero, N. B., Mercuri, E., Voit, T., Sewry, C. A., Guicheney, P., and Muntoni, F. (2001) *Am. J. Hum. Genet.* **69**, 1198–1209
- Longman, C., Brockington, M., Torelli, S., Jimenez-Mallebrera, C., Kennedy, C., Khalil, N., Feng, L., Saran, R. K., Voit, T., Merlini, L., Sewry, C. A., Brown, S. C., and Muntoni, F. (2003) *Hum. Mol. Genet.* **12**, 2853–2861
- Jimenez-Mallebrera, C., Brown, S. C., Sewry, C. A., and Muntoni, F. (2005) *Cell. Mol. Life Sci.* **62**, 809–823
- Michele, D. E., Barresi, R., Kanagawa, M., Saito, F., Cohn, R. D., Satz, J. S., Dollar, J., Nishino, I., Kelley, R. L., Somer, H., Straub, V., Mathews, K. D., Moore, S. A., and Campbell, K. P. (2002) *Nature* **418**, 417–422
- Ervasti, J. M., and Campbell, K. P. (1991) *Cell* **66**, 1121–1131
- Stalnaker, S. H., Hashmi, S., Lim, J. M., Aoki, K., Porterfield, M., Gutierrez-Sanchez, G., Wheeler, J., Ervasti, J. M., Bergmann, C., Tiemeyer, M., and Wells, L. (2010) *J. Biol. Chem.* **285**, 24882–24891
- Nakamura, N., Stalnaker, S. H., Lyalin, D., Lavrova, O., Wells, L., and Panin, V. M. *Glycobiology* **20**, 381–394
- Manya, H., Chiba, A., Yoshida, A., Wang, X., Chiba, Y., Jigami, Y., Margolis, R. U., and Endo, T. (2004) *Proc. Natl. Acad. Sci. U.S.A.* **101**, 500–505
- Combs, A. C., and Ervasti, J. M. (2005) *Biochem. J.* **390**, 303–309
- Yoshida-Moriguchi, T., Yu, L., Stalnaker, S. H., Davis, S., Kunz, S., Madison, M., Oldstone, M. B., Schachter, H., Wells, L., and Campbell, K. P. (2010) *Science* **327**, 88–92
- Chai, W., Yuen, C. T., Kogelberg, H., Carruthers, R. A., Margolis, R. U., Feizi, T., and Lawson, A. M. (1999) *Eur. J. Biochem.* **263**, 879–888
- Aoki, K., Perlman, M., Lim, J. M., Cantu, R., Wells, L., and Tiemeyer, M. (2007) *J. Biol. Chem.* **282**, 9127–9142
- Aoki, K., Porterfield, M., Lee, S. S., Dong, B., Nguyen, K., McGlamry, K. H., and Tiemeyer, M. (2008) *J. Biol. Chem.* **283**, 30385–30400
- Liu, J., Ball, S. L., Yang, Y., Mei, P., Zhang, L., Shi, H., Kaminski, H. J., Lemmon, V. P., and Hu, H. (2006) *Mech. Dev.* **123**, 228–240
- Kanagawa, M., Saito, F., Kunz, S., Yoshida-Moriguchi, T., Barresi, R., Kobayashi, Y. M., Muschler, J., Dumanski, J. P., Michele, D. E., Oldstone, M. B., and Campbell, K. P. (2004) *Cell* **117**, 953–964
- Moore, S. A., Saito, F., Chen, J., Michele, D. E., Henry, M. D., Messing, A., Cohn, R. D., Ross-Barta, S. E., Westra, S., Williamson, R. A., Hoshi, T., and Campbell, K. P. (2002) *Nature* **418**, 422–425
- Ciucanu, I., and Kerek, F. (1984) *Carbohydr. Res.* **131**, 209–217
- Bax, A., and Summers, M. (1986) *J. Am. Chem. Soc.* **108**, 2093–2094
- Podlasek, C., Wu, J., Stripe, W., Bondo, P., and Serianni, A. S. (1995) *J. Am. Chem. Soc.* **117**, 8635–8644
- Bubb, W. A. (2003) *Concepts Magn. Reson. Part A* **19A**, 1–19
- Michele, D. E., and Campbell, K. P. (2003) *J. Biol. Chem.* **278**, 15457–15460
- Cao, W., Henry, M. D., Borrow, P., Yamada, H., Elder, J. H., Ravkov, E. V., Nichol, S. T., Compans, R. W., Campbell, K. P., and Oldstone, M. B. (1998) *Science* **282**, 2079–2081
- Spiropoulou, C. F., Kunz, S., Rollin, P. E., Campbell, K. P., and Oldstone, M. B. (2002) *J. Virol.* **76**, 5140–5146
- Endo, T. (1999) *Biochim. Biophys. Acta* **1473**, 237–246
- Alvarez-Manilla, G., Troupe, K., Fleming, M., Martinez-Urbe, E., and Pierce, M. *Glycobiology* **20**, 166–174
- Chiba, A., Matsumura, K., Yamada, H., Inazu, T., Shimizu, T., Kusunoki, S., Kanazawa, I., Kobata, A., and Endo, T. (1997) *J. Biol. Chem.* **272**, 2156–2162
- Sutton-Smith, M., Morris, H. R., Grewal, P. K., Hewitt, J. E., Bittner, R. E., Goldin, E., Schiffmann, R., and Dell, A. (2002) *Biochem. Soc. Symp.* **69**, 105–115

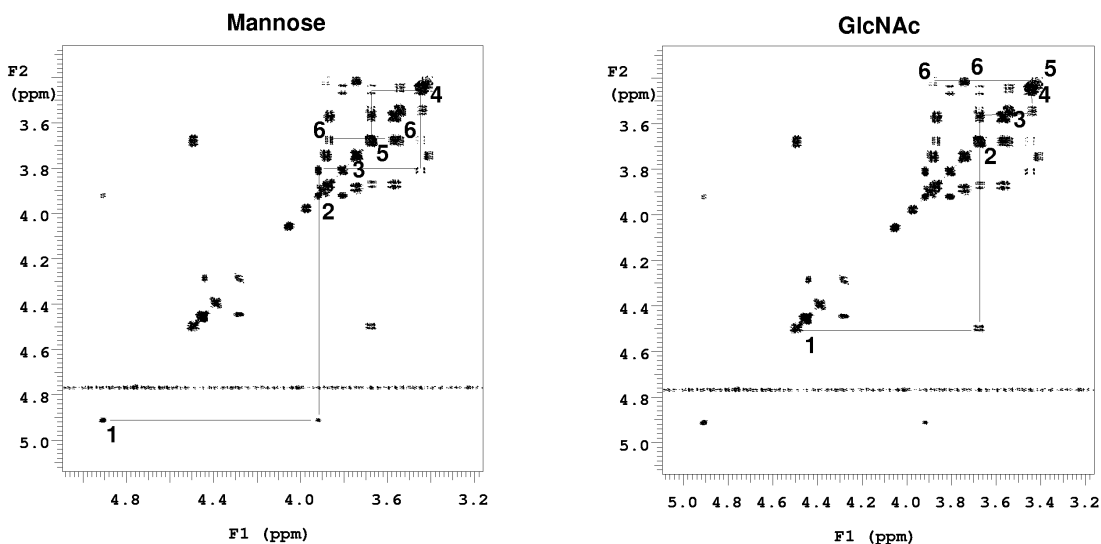


Figure S1. Double-quantum filtered COSY spectrum of Ac-YVEP(GlcNAc- β -1,2-Man α -)TAV-NH₂ with the connectivity for the protons in the Mannose and GlcNAc residues indicated.

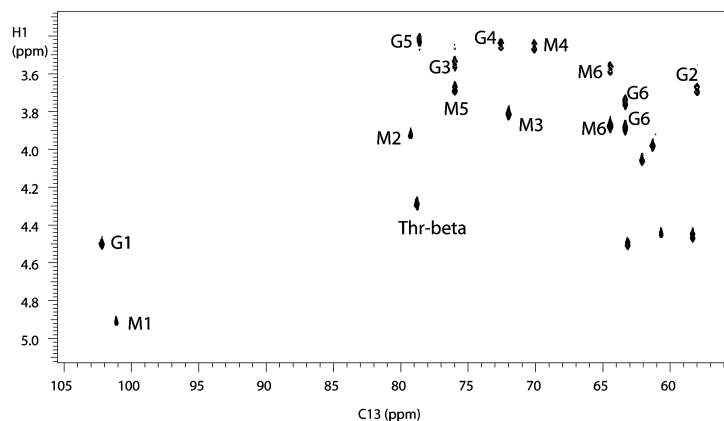


Figure S2. Region containing the carbohydrate resonances of the ¹H-¹³C HMQC spectrum of Ac-YVEP(GlcNAc- β -1,2-Man α -)TAV-NH₂ with crosspeaks for directly bonded H,C pairs assigned. (M=mannose, G=GalNAc) Unlabeled cross peaks arise from amino acid residues.

Table S1. Chemical shifts ($^1\text{H}/^{13}\text{C}$) for disaccharide glycan components and linking threonine β . Chemical shifts are relative to DSS.

1	2	3	4	5	6
Mannose					
4.91/101.20	3.91/79.31	3.80/72.07	3.44/70.13	3.67/76.06	3.57,3.87/64.42
GlcNAc					
4.49/102.24	3.68/58.07	3.54/76.07	3.44/72.59	3.42/78.67	3.74,3.88/63.39
Thr beta					
4.28/78.84					